American Mineralogist, Volume 62, pages 151–157, 1977

The spectra of iron in orthopyroxene revisited: the splitting of the ground state[1]

DON S. GOLDMAN AND GEORGE R. ROSSMAN

Division of Geological and Planetary Sciences
California Institue of Technology
Pasadena, California 91125

Abstract

The optical absorption spectra of Fe^{2+} in the $M(2)$ site of orthopyroxene have been reanalyzed, in view of the experimental observation of a mid-infrared band at 2350 cm^{-1} arising from an electronic transition within the split $^5T_{2g}$ ground state of the low-symmetry site. This analysis uses C_{2v} spectroscopic symmetry and a crystal-field potential which includes fourth-order harmonic terms. The order of the energy states is found to depend upon specific bond angles and lengths. The 2350 cm^{-1} band is assigned as a transition to the $^5B_2$ state, calculated to lie above the $^5A_2$ state. This result indicates that the entire splitting of the $^5T_{2g}$ ground state is 2350 cm^{-1}.

Introduction

The electronic absorption spectrum of ferrous iron in the $M(2)$ site of orthopyroxene, $(Mg,Fe)SiO_3$, has been the subject of many investigations aimed at understanding the polarization properties and splittings among the various bands that result from iron in a low-symmetry, coordination environment. White and Keester (1966) assigned a band at 11,000 cm^{-1} in the spectrum of enstatite to Fe^{2+} in octahedral coordination, and assigned a band at about 5400 cm^{-1} to Fe^{2+} in tetrahedral coordination. It was subsequently suggested by Bancroft and Burns (1967) and later accepted by White and Keester (1967) that both bands arise from Fe^{2+} in the distorted, six-coordinate $M(2)$ site. Runciman *et al.* (1973) pointed out an incorrect classification of C_{2v} states used in the previous studies to explain the polarization properties of these bands. They presented spectra of enstatite and analyzed the results in a crystal-field analysis that was also based upon a C_{2v} model, but with a different classification of states. Because of the large energy splittings and the polarization characteristics exhibited by these bands, the spectra of Fe^{2+} in the $M(2)$ site of orthopyroxene are used as the model for the study of the spectra of iron in a variety of low-symmetry environments.

The degeneracies within the octahedral $^5T_{2g}$ and ^5E_g states of Fe^{2+} are removed in C_{2v} symmetry, producing five states, among which a maximum of three allowed electric dipole transitions are possible, depending upon the symmetry of the ground state. For this reason, a third absorption band was sought in previous studies. White and Keester (1966) observed a band at 3100 cm^{-1} and attributed it to a vibrational overtone of the silicate lattice. Bancroft and Burns (1967) assigned this band to Fe^{2+} in the $M(2)$ site. Runciman *et al.* determined the polarization properties of a band at 3100 cm^{-1} and also assigned it to Fe^{2+} in the $M(2)$ site.

It was pointed out by Goldman and Rossman (1976) that the half-width of the 3100 cm^{-1} band is an order of magnitude smaller than the other $M(2)$ Fe^{2+} bands. This suggested a vibrational origin and led them to examine a number of orthopyroxenes to determine the origin of this band. It was found that this band does not arise from $M(2)$ Fe^{2+}. In the course of that investigation, they found a band at 2350 cm^{-1} which correlated with $M(2)$ Fe^{2+} content, had the correct polarization properties for the C_{2v} model proposed by Runciman *et al.*, and had a half-width similar to those of the other $M(2)$ Fe^{2+} bands. Thus, the crystal-field analysis of the orthopyroxene spectral data of Runciman *et al.* is quantitatively incorrect, due to the incorporation of the incorrectly assigned 3100 cm^{-1} band.

Orthopyroxene is the only documented sample in which all three C_{2v} allowed transitions are observed.

[1] Contribution No. 2713

In addition, it is the only sample in which a mid-infrared absorption band of Fe^{2+} within the split ${}^5T_{2g}$ ground state has been confirmed. Therefore, it is essential to quantitatively understand these data. For this reason, the orthopyroxene spectral data will be reanalyzed with a quantitatively different C_{2v} point-charge model. It will be shown that this model results in a more acceptable and understandable energy-level scheme while still explaining the observed absorption anisotropy of the various bands.

Experimental method

Self-supporting sections of bronzite from Bamble, Norway, were cut parallel and perpendicular to c, using external crystal morphology for orientation. An additional (001) section was set in epoxy on a microscope slide, thinned and polished to about 100 μm for measurement of the intense α band at 930 nm. The thickness of this section was determined by removing the sample from the epoxy and measuring it directly. Euhedral crystals, tabular along (100), of a hypersthene from Summit Rock, Oregon (Kleck, 1970) were sufficiently thin so that only polishing was necessary prior to obtaining their spectra. The orientation in all cases was confirmed by conoscopic interference figures. All spectra presented herein were obtained at room temperature, although the mid-infrared spectra of the Bamble bronzite were also obtained at 12°K using a Cryogenic Technology, Inc. cryogenic refrigerator. Other experimental details are similar to those presented in Rossman (1975 a,b). Chemical analyses were obtained with an automated MAC5-SA3 electron microprobe using the technique of Bence and Albee (1968) for data reduction (Table 1).

TABLE 1. Microprobe analyses

SAMPLE	1	2
	Weight Percent of Oxides	
SiO_2	57.83	53.30
TiO_2	-	.19
Al_2O_3	.09	.23
MgO	32.86	19.67
MnO	-	.51
FeO	9.77	25.02
CaO	.26	1.76
	100.81	100.68
	Formula Proportions (#cations = 4)	
Si	2.00	2.00
Al(VI)	-	.01
Mg	1.70	1.10
Ti	-	.01
Mn	-	.02
Fe	.28	.79
Ca	.01	.07

1. Bronzite, Bamble, Norway
2. Hypersthene, Summit Rock, Oregon

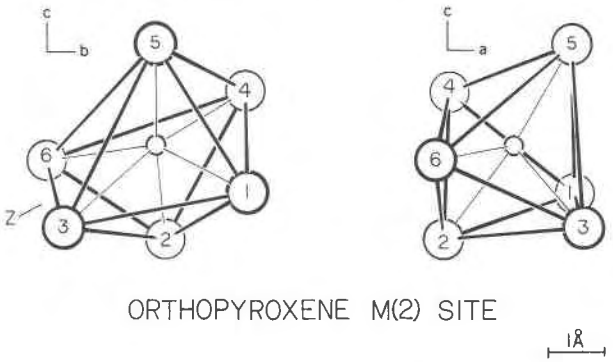

FIG. 1. (100) and (010) ORTEP projections of the $M(2)$ coordination site in orthopyroxene (hypersthene) based upon the atomic coordinates given by Ghose (1965). Both projections are drawn to the same scale.

Each spectrum and its polarized baseline was digitized, using a Calma X-Y digitizer. A plotting program was written for the IBM 370/155 to correct each spectrum for its polarizer baseline, to normalize the intensity to represent a desired crystal thickness, and to plot a smooth curve through all data points using a second-order polynomial interpolation function.

Crystal structure and optical orientation

Ghose (1965) analyzed the crystal structure of a hypersthene, $Mg_{0.93}Fe_{1.07}Si_2O_6$, with space-group *Pbca*: a = 18.310, b = 8.927, and c = 5.226 Å. The optical orientation is $\alpha = b$, $\beta = a$, and $\gamma = c$. All atoms have C_1 point-group symmetry. (100) and (010) ORTEP (Johnson, 1965) projections of the $M(2)$ site are presented in Figure 1. The position of the metal ion in Figure 1 represents an $M(2)$ site that contains 90 percent Fe^{2+}. The principal distortion of this site from octahedral geometry results from an elongation of the $M(2)$–O(6) and $M(2)$–O(3) bonds with a reduction in the O(6)–$M(2)$–O(3) angle to 72.2°.

Spectroscopic data

The room-temperature spectra of the Bamble bronzite are presented in the 15000–4000 cm^{-1} region in Figure 2 to illustrate the absorption bands due to Fe^{2+} in the $M(2)$ site. Bancroft and Burns (1967) and Burns (1970) reported room-temperature, polarized spectra in the 25000–4000 cm^{-1} region of a bronzite sample from this locality, and the reader is referred to these studies for the spectroscopic details that occur

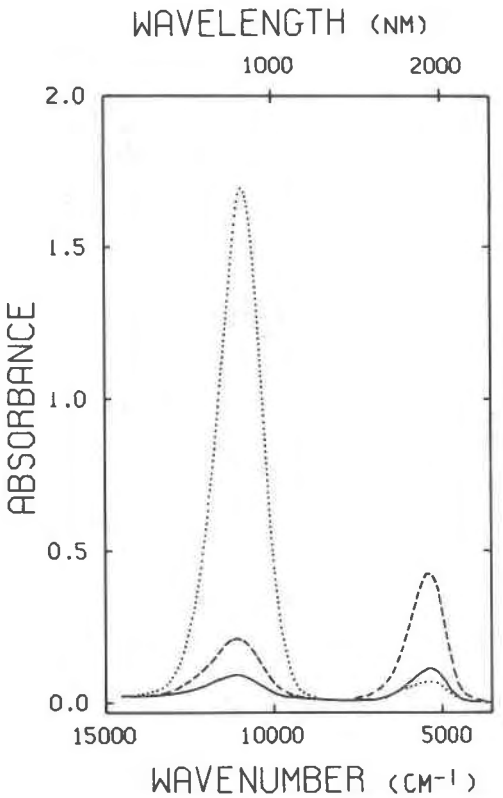

FIG. 2. Room temperature spectra of bronzite ($Fs_{14.0}$) from Bamble, Norway illustrating the absorption bands due to Fe^{2+} in the $M(2)$ site. ..... α spectrum; ----β spectrum; ———— γ spectrum. Crystal thickness = 0.10 mm. Optic orientation: $\alpha = b, \beta = a, \gamma = c$.

above 15000 cm^{-1}. Mössbauer analysis of that sample (Bancroft *et al.*, 1967) indicated that greater than 90 percent of the total Fe^{2+} is in the $M(2)$ site. In fact, a quadrupole-split doublet due to Fe^{2+} in $M(1)$ was not detected. The spectra in Figure 2 differ[2] from those previously reported in the intensities of the α, β, and γ components of the band at 11,000 cm^{-1}.

The band in the mid-infrared at 2350 cm^{-1} (Fig. 3) is assigned to Fe^{2+} in the $M(2)$ site. Runciman *et al.* indicated that a mid-infrared band due to Fe^{2+} in this site must be polarized mostly in γ to conform to a C_{2v} point-group, which explains the α and β-polarized bands at 11,000 cm^{-1} and 5400 cm^{-1}, respectively. The α, β and γ spectra of the Bamble bronzite have been obtained at 12°K to determine the polarization ratios for the 2350 cm^{-1} band. The low temperature diminishes the overlap of the 2350 cm^{-1} band with the vibrational overtones that occur below 2200 cm^{-1} so that more accurate intensity ratios can be obtained. The resulting ratios for the α, β, and γ bands at 2350 cm^{-1} are 0.28:0.20:0.52. Therefore, this band is predominantly γ-polarized with some α and some β due to the different orientations of the C_{2v} crystal-field axes and the principal optical directions, as will be discussed in the next section. Coincidentally, these polarization ratios are nearly identical to the ratios determined for the 3100 cm^{-1} band by Runciman *et al.*, which were used to compare the theoretical intensities calculated from the selected C_{2v} crystal-field axes with the experimental intensities.

Point group and band assignments

The crystallographic point-group symmetry of the $M(2)$ site is C_1. In this point group, all transitions are allowed in each polarization. However, the 11,000 cm^{-1}, 5400 cm^{-1}, and 2350 cm^{-1} bands are strongly polarized, indicating that the Fe^{2+} ion experiences an effective electrostatic symmetry higher than C_1. Runciman *et al.* developed a model based upon C_{2v} symmetry, and noted errors made in earlier studies in the assignment of absorption bands to specific transitions of Fe^{2+}. This process utilizes the descent-in-symmetry method from O_h to D_{4h} to C_{2v}. Problems arose because the assignment of experimentally-determined energy values to the specific symmetry states of C_{2v} by reducing the overall symmetry from D_{4h} is not unique and depends upon the type of rhombic distortion. There are four types of rhombic distortions that can

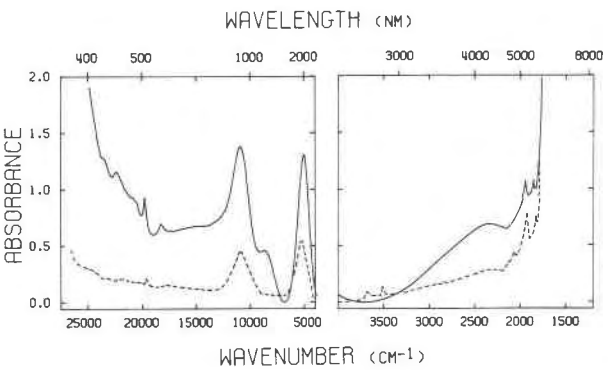

FIG. 3. Room temperature γ spectrum (————) of hypersthene ($Fs_{39.5}$) from Summit Rock, Oregon, and the γ spectrum (------) of bronzite ($Fs_{14.0}$) from Bamble, Norway which indicate that the bands at 5400 cm^{-1} and at 2350 cm^{-1} are correlated in intensity and arise from Fe^{2+} in the $M(2)$ site. Crystal thickness = 0.50 mm.

[2] These differences arise from the nature of the experimental methods used to obtain the spectra. The spectra of Bancroft and Burns (1967) and Burns (1970) were obtained with microscope spectrophotometers which necessarily mix polarization components due to the strongly convergent light in the optical system. The quantitative aspects of this problem will be dealt with in a forthcoming paper.

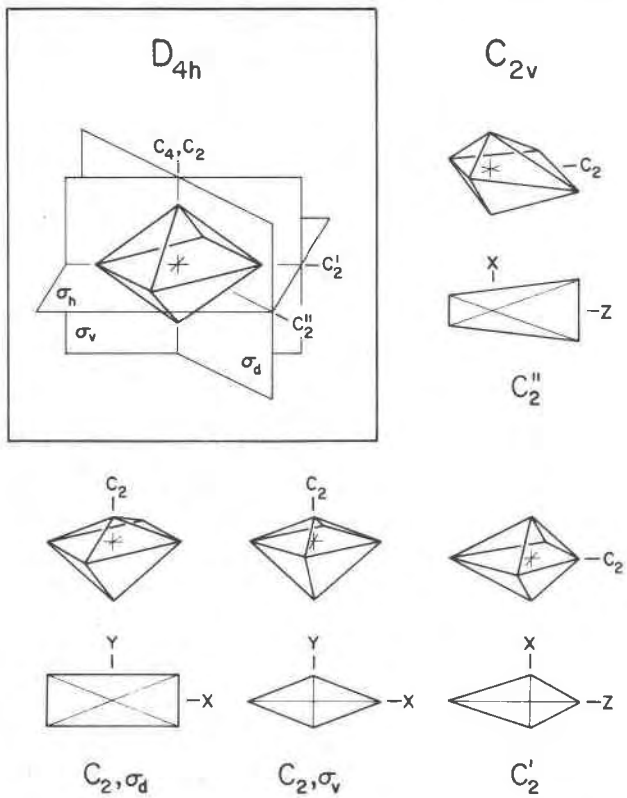

Fig. 4. Four types of C_{2v} polyhedra resulting from rhombic distortions of a D_{4h} polyhedron. Each C_{2v} figure is designated by the only symmetry elements that remain from D_{4h}. For each C_{2v} figure, the sections viewed along the former C_4 axis of D_{4h} and the X,Y,Z axes are also shown where Z corresponds to the two-fold rotation axis.

be applied to a D_{4h} polyhedron, each resulting in a distinct C_{2v} polyhedron whose symmetry elements (a two-fold rotation axis and two mirror planes) are related differently to the original symmetry elements of the D_{4h} polyhedron. Figure 4 illustrates the four C_{2v} types, in which each type is designated by the only symmetry elements that remain from D_{4h} (Wilson *et al.*, 1955). In addition, the section of each C_{2v} type viewed along the former C_4 axis of D_{4h} is presented to facilitate a comparison of the distortions.

Idealized energy-level schemes for each C_{2v} type have been constructed from the correlation tables in Wilson *et al.* and are presented in Figure 5, in which the descent-in-symmetry from O_h to C_{2v} is given. The polarization properties of the allowed transitions have been determined using the character table for C_{2v} in Cotton (1963).

The appropriate C_{2v} model for the $M(2)$ site is C_2'', due to the orientation of an approximate two-fold rotation axis between the O(1)–O(4) and O(6)–O(3) oxygen pairs. The XZ plane of $C_{2v}(C_2'')$ symmetry (Fig. 4) was approximated in the orthopyroxene $M(2)$ coordination polyhedron by the $M(2)$ metal ion and the O(1), O(3), O(4) and O(6) oxygens (Runciman *et al.*) Hence, the 11,000cm^{-1}, 5400cm^{-1}, and 2350cm^{-1} absorption bands are assigned from Figure 5 to the $A_1 \rightarrow A_1$, $A_1 \rightarrow B_1$ and $A_1 \rightarrow B_2$ transitions of Fe^{2+} in the $M(2)$ site. Each of these transitions is allowed in only one of the crystal-field directions. However, the crystal-field directions are not aligned with the principal vibration directions of the indicatrix. Therefore, components of each transition will occur in all vibration directions, but the transitions to A_1, B_1, and B_2, polarized in Z, X, and Y, are expected to occur mostly in α, β, and γ, respectively.

Runciman *et al.* (Table 1, set 1) calculated theoretical intensity ratios of the α, β, and γ components for these transitions of 0.85:0.02:0.14, 0.05:0.67:0.29, and 0.10:0.33:0.58, respectively. Our measured ratios for the Bamble bronzite for these bands are 0.86:0.10:0.04, 0.11:0.70:0.19, and 0.28:0.20:0.52, respectively. The general agreement between the theoretical and experimental intensity ratios for the three $M(2)$ Fe^{2+} bands is certainly suggestive of a C_{2v} spectroscopy. These data could not be explained using either C_1 or C_2 point-group symmetry.

Upon considering the orientation of the five d orbitals in each of the C_{2v} polyhedra in Figure 4, a

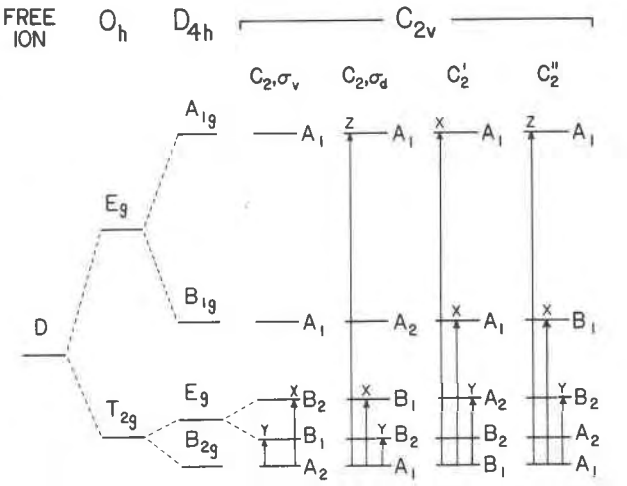

FIG. 5. Correlation diagram showing the idealized descent-in-symmetry from O_h to C_{2v}. The polarization properties of the allowed transitions represent the axial labelings and the distortions presented in Fig. 4. The effect of configuration interaction between the two A_1 states in C_{2v} symmetry is ignored. Also, tetragonal compression between O_h and D_{4h} and the barycenter "rule" for the split states are assumed. $C_{2v}(C_2'')$ is applicable to the orthopyroxene M(2) site.

general ordering scheme of the various states is readily obtained. For instance, by assuming tetragonal compression between O_h and D_{4h} (Fig. 5), A_{1g} is expected to be at higher energy than B_{1g} in D_{4h} symmetry. As a consequence, A_1 is expected to be at higher energy than B_1 in $C_{2v}(C_2'')$. In the same manner, the energy level of the two C_{2v} states derived from the E_g state of D_{4h} were obtained for the distortions presented in Figure 4. Generally, the relative energy levels of these states are reversed if (1) the elongation in the XY plane is along Y in C_2, σ_v; (2) the dihedral angle about X is greater than 90° in C_2, σ_d; (3) the elongation in the XZ plane is along X in C_2'; and (4) the dihedral angle about Z is greater than 90° in C_2''.

The O(3)–M(2)–O(6) and O(1)–M(2)–O(4) angles about the crystal-field Z axis of the M(2) site are both less than 90°. Therefore, A_2 is expected to be at a lower energy than B_2 from the arguments presented above. However, Runciman *et al.* calculated just the reverse. This discrepancy will be examined in the following section.

Crystal field analysis

The general crystal-field treatment described by Runciman *et al.* will be used to analyze the spectra of bronzite presented in this paper in light of the assignment of a third C_{2v} band of Fe^{2+} in the M(2) site at 2350 cm^{-1}. However, it will be shown that this method does not result in a satisfactory energy-level scheme, and for this reason, the bronzite data will be reanalyzed using a different crystal-field treatment. First, it is helpful to review the pertinent aspects of the crystal-field method of Runciman *et al.*

Runciman *et al.* derived a crystal-field potential using a $C_{2v}(C_2'')$ model. Fourth and higher order harmonic terms were excluded from the potential, after extracting octahedral terms, because an exact solution for their coefficients would require more data than are available in the spectra. Hence, Δ and two additional fitting parameters that relate to the coefficients of the Y_2^0 and $Y_2^{\pm 2}$ harmonic terms were fitted. $\Delta(10D_q)$ refers to the energy separation between the octahedral $^5T_{2g}$ and ^5E_g states initially needed to produce the observed splittings of the C_{2v} states, and which also accounts for the effect of configuration interaction between the two A_1 states. It is important to realize that this method does not incorporate the specific bond-length and bond-angle distortions of the C_{2v} site within the potential, and therefore does not distinguish between sites of different $C_{2v}(C_2'')$ coordination geometries.

The values of Δ and of the forbidden $A_1 \rightarrow A_2$ transition have been calculated from the energy expressions given in Runciman *et al.*, using the following bronzite data from Figures 2 and 3: $A_1 \rightarrow A_1$ = 10930 cm^{-1}; $A_1 \rightarrow B_1$ = 5400 cm^{-1}, and $A_1 \rightarrow B_2$ = 2350 cm^{-1}. The energy values of Δ and of the $A_1 \rightarrow A_2$ transition are calculated to be 4934 cm^{-1} and 6178 cm^{-1}, respectively. These results indicate that the splitting of the $^5T_{2g}(O_h)$ state is also 6178 cm^{-1}, because B_2 is at lower energy than A_2. However, from the discussion in the previous section, a dihedral angle about Z of less than 90° leads to the prediction that A_2 is at lower energy than B_2. As will be shown subsequently, A_2 transforms as an XY wavefunction in $C_{2v}(C_2'')$ and B_2 transforms as a YZ wavefunction. An acute dihedral angle about Z increases the potential about YZ relative to XY, and thus A_2 is expected to lie beneath B_2. Therefore, the O(6)–M(2)–O(3) angle of 72.2° and the O(1)–M(2)–O(4) angle of 83° suggest that the energy level scheme resulting from the method of Runciman *et al.* is incorrect. For this reason, the bronzite data will be reanalyzed, using a crystal-field treatment that incorporates fourth-order contributions of the distortion into the potential and also considers the effect of specific bond lengths and angles.

The bronzite data have been reanalyzed[3] using the operator-equivalent method described in Hutchings (1964) to derive energy expressions for the various $C_{2v}(C_2'')$ states using the Z axis in Figure 1 as the axis of quantization. Contributions from the Y_2^0, $Y_2^{\pm 2}$, Y_4^0, $Y_4^{\pm 2}$, $Y_4^{\pm 4}$ harmonic terms remain in the potential after subtracting the octahedral terms. The number of fitting parameters in addition to Δ are reduced to two by deriving the potential in terms of one specified bond length, which in this case is taken to be the average metal–oxygen distance, $\bar{a}$; one fitting parameter is related to the second-order terms and the other is related to the fourth-order terms. The method assumes that each ligand constitutes a point charge. Hence, there are three fitting parameters, and the spectra can be analyzed as before. The potential, written in operator-equivalent notation, consists of an octahedral term, Δ, and

$$M\left[\frac{A}{3}\hat{O}_2^0 + B\hat{O}_2^2\right] + N\left[\frac{C}{8}\hat{O}_4^0 + 5D\hat{O}_4^2 + \frac{35E}{4}\hat{O}_4^4\right]$$

[3] A detailed description of the crystal-field method used in this paper can be obtained by ordering Document AM-76-035 from the Business Office, Mineralogical Society of America, 1909 K Street, N.W., Washington, D. C. 20006. Please remit $1.00 in advance for the microfiche.

TABLE 2. C_{2v} crystal-field levels

State	Wavefunction	Energy
B_1	$\sqrt{3}XZ$	$-M(A+3B) - 6N(C-10D) + 0.6\Delta$
B_2	$\sqrt{3}YZ$	$M(3B-A) - 6N(C+10D) - 0.4\Delta$
A_2	$\sqrt{3}XY$	$2AM + \frac{3}{2}N(C-70E) - 0.4\Delta$

where

$$M = \frac{-q\langle r^2\rangle}{14\bar{a}^3} \qquad N = \frac{q\langle r^4\rangle}{504\bar{a}^5}$$

$\hat{O}_2^0$, $\hat{O}_2^2$, $\hat{O}_4^0$ and $\hat{O}_4^4$ are the operator equivalents of the associated spherical harmonic terms, and A, B, C, D, and E are determined by the bond angles and bond lengths of the site. The $M(2)$ site possesses six unequal metal–oxygen bond lengths, from which three bond lengths must be selected to conform to a C_{2v} point-group symmetry. Therefore, the averages of the following bond lengths are used: $M(2)$–O(6), $M(2)$–O(3); $M(2)$–O(1), $M(2)$–O(4), and $M(2)$–O(2), $M(2)$–O(5).

The energy expressions for the two A_1 states are the eigenvalues of the following configuration interaction matrix:

$$\begin{array}{cc} \langle d_{yz}\rangle & \langle d_{(x^2-z^2)}\rangle \\ \begin{bmatrix} M(A+3B) + \frac{9}{8}N(3C+40D+70E) + 0.6\Delta & M(B-A)\sqrt{3} + N(C+8D-14E)\,\frac{15}{8}\sqrt{3} \\ M(B-A)\sqrt{3} + N(C+8D-14E)\,\frac{15}{8}\sqrt{3} & -M(A+3B) + \frac{3}{8}N(19C-120D+70E) - 0.4\Delta \end{bmatrix} & \end{array}$$

Table 2 lists the wavefunctions and energies of the other three states.

The solutions for the bronzite data are: $\Delta = 6522$ cm^{-1}; $A_1 \rightarrow A_2 = 354$ cm^{-1}; $M = -636$ cm^{-1}, and $N = 9.5$ cm^{-1}. The energy-level scheme based upon these calculations is presented in Figure 6. As predicted from the acute dihedral angles about Z for the $M(2)$ site, the energy level of A_2 is calculated below B_2 and the overall splitting of the $^5T_{2g}(O_h)$ state, determined by the $A_1 \rightarrow B_2$ transition energy, is only 2350 cm^{-1}. This splitting of the $^5T_{2g}(O_h)$ state, much smaller than previously calculated, supports the contention by Faye (1972) that the splitting of this state is either small or nearly the same for a large variety of mineral spectra. It is unlikely that Faye's suggestion can be accurately tested below 2000 cm^{-1}, due to the presence of vibrational absorptions in that region. However, the identification of the Fe^{2+} band at 2350 cm^{-1} represents the largest confirmed splitting of the $^5T_{2g}(O_h)$ ground state known to us. Also, the magnitude of splitting indicated by this band arises from one of the largest, distorted six-coordinate mineral sites. These observations suggest that the splitting of the $^5T_g(O_h)$ state is probably not greater than 2000 cm^{-1} is most minerals, although further data are needed, especially in the 2000–4000 cm^{-1} region, to examine this possibility further.

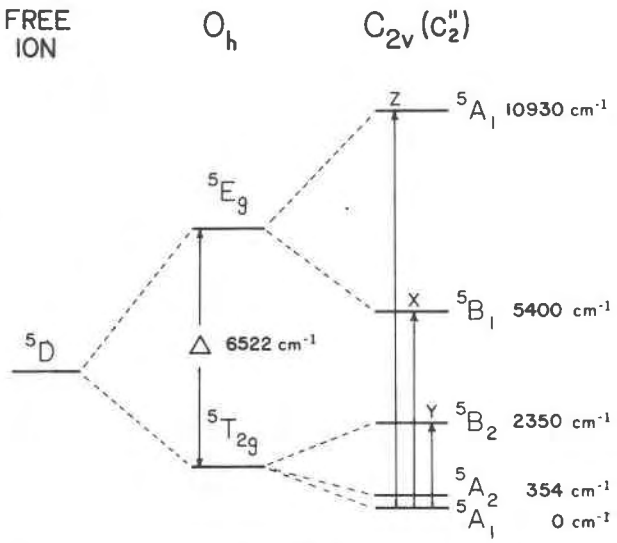

FIG. 6. Energy level scheme of Fe^{2+} in the $M(2)$ site using a $C_{2v}(C_2'')$ theoretical point-charge model.

The calculated value of Δ for Fe^{2+} in the $M(2)$ site is 6522 cm^{-1}. This value is reasonable, considering the dependence of Δ on $1/\bar{a}^5$ (Figgis, 1966). To determine a value of Δ for Fe^{2+} in a more regular, six-coordinate site so that the $1/\bar{a}^5$ dependence can be evaluated for the bronzite data, use is made of a study conducted by Faye (1972). Faye indicated that the barycenter energy of the states derived from the splitting of the $^5E_g(O_h)$ state is approximately 10,000 cm^{-1} for many six-coordinate sites (*i.e.*, the $M(1)$ sites in orthopyroxene, *etc.*) which have $\bar{a}$ values of about 2.1 Å. Since the barycenter energy is determined by the transitions from the ground state, any splitting of the $^5T_{2g}(O_h)$ states results in a barycenter energy that is larger than Δ (see Fig. 6). Therefore, assuming that a Δ of 9500 cm^{-1} is produced from a site with $\bar{a} = 2.1$ Å, a $1/\bar{a}^5$ dependence predicts a Δ of about 7200 cm^{-1} for Fe^{2+} in the orthopyroxene $M(2)$ site, using 2.22 Å for $\bar{a}$ (Ghose, 1965). Although there appears to be general agreement between the values of Δ calculated from the spectral data and from the

$1/\bar{a}^5$ dependence, it should be realized that this dependence assumes octahedral geometry. The validity of calculating a value for Δ based upon the average of six M–O bonds lengths in a distorted coordination site is subject to question, especially when four M–O bonds are typically 2.1 Å in length, whereas the remaining two bonds are extremely long at greater than 2.4 Å. However, using $\bar{a}$ in these calculations may be the most appropriate way in which the analysis of the spectral data from distorted coordination sites can be compared. From the analysis of the bronzite spectra, it is concluded that by incorporating the fourth-order contributions into the potential and by considering the effect of bond-length and bond-angle distortions of the $M(2)$ site, a more reasonable C_{2v} energy level scheme is obtained which still explains the polarization properties of the various bands.

Finally, it must be pointed out that the β and γ components of the bands near 11,000 cm^{-1} and the α and γ components of the band near 5400 cm^{-1} do not occur at the same energy at which the main components occur (Fig. 2). These differences may result from weak spin-orbit coupling interactions. Ham *et al.* (1969) in a study of Fe^{2+} doped into octahedrally-coordinated sites in MgO suggested that spin-orbit interactions, affected by Jahn-Teller distortions, produce a splitting of the ${}^5T_{2g}$ state of approximately 100 cm^{-1}. Runciman *et al.* pointed out that spin-orbit splittings of Fe^{2+} in the $M(2)$ site are expected to be small, due to a quenching effect of a low-symmetry environment. It is therefore conceivable that the small differences ($\sim$100 cm^{-1}) in the energy locations of the various components of the band near 11,000 cm^{-1} and 5400 cm^{-1} are due to spin-orbit interactions, although more data are required to evaluate this possibility.

Acknowledgments

We are indebted to Jeff Hare, Caltech, for numerous discussions concerning the point charge calculations and crystal-field interpretations of the orthopyroxene spectra. We thank Jack Huneke for the hypersthene sample from Oregon.

References

BANCROFT, G. M. AND R. G. BURNS (1967) Interpretation of the electronic spectra of iron in pyroxenes. *Am. Mineral.* **52,** 1278–1287.

———, ——— AND R. A. HOWIE (1967) Determination of the cation distribution in the orthopyroxene spectra by the Mössbauer effect. *Nature,* **213,** 1221–1223.

BENCE, A. E. AND A. L. ALBEE (1968) Empirical correction factors for the electron microanalysis of silicate and oxides. *J. Geol.* **76,** 382–403.

BURNS, R. G. (1970) *Mineralogical Applications of Crystal Field Theory.* Cambridge University Press, Cambridge, England.

COTTON, F. A. (1963) *Chemical Applications of Group Theory.* Wiley-Interscience, New York.

FAYE, G. H. (1972) Relationship between crystal-field splitting parameter, "Δ_{VI}", and M_{host}–O bond distance as an aid in the inerpretation of absorption spectra of Fe^{2+}-bearing materials, *Can. Mineral.* **11,** 473–487.

FIGGIS, B. N. (1966) *Introduction to Ligand Fields.* Interscience Publishers, New York.

GHOSE, S. (1965) Mg^{2+}–Fe^{2+} order in an orthopyroxene, $Mg_{0.93}Fe_{1.07}Si_2O_6$. *Z. Kristallogr.* **122,** 81–99.

GOLDMAN, D. S. AND G. R. ROSSMAN (1976) Identification of a mid-infrared electronic absorption band of Fe^{2+} in the distorted $M(2)$ site of orthopyroxene, $(Mg,Fe)SiO_3$. *J. Chem. Phys. Lett.,* **41,** 474–475.

HAM, F. S., W. M. SCHWARZ AND M. C. M. O'BRIEN (1969) Jahn-Teller effects in the far-infrared, EPR, and Mössbauer spectra of MgO:Fe^{2+}. *Phys. Rev.* **185,** 548–567.

HUTCHINGS, M. T. (1964) Point-charge calculations of energy levels of magnetic ions in crystalline electric fields. *Solid State Phys.* **16,** 227–273.

JOHNSON, C. K. (1965) ORTEP:FORTRAN thermal ellipsoid plot program for crystal structure illustrations. Report ORNL-**3794,** Oak Ridge National Laboratory, Oak Ridge, Tennessee.

KLECK, W. C. (1970) Cavity minerals at Summit Rock, Oregon. *Am. Mineral.* **55,** 1396–1404.

ROSSMAN, G. (1975a) Joaquinite: The nature of its water content and the question of four-coordinated ferrous iron. *Am. Mineral.* **60,** 435–440.

——— (1975b) Spectroscopic and magnetic studies of ferric iron hydroxy sulfates: intensification of color in ferric iron clusters bridged by a single hydroxide ion. *Am. Mineral.* **60,** 698–704.

RUNCIMAN, W. A., D. SENGUPTA AND M. MARSHALL (1973) The polarized spectra of iron in silicates. I. Enstatite. *Am. Mineral.* **58,** 444–450.

WHITE, W. B. AND K. L. KEESTER (1966) Optical absorption spectra of iron in the rock-forming silicates. *Am. Mineral.* **51,** 774–791.

——— AND ———(1967) Selection rules and site assignments for the spectra of ferrous iron in pyroxenes. *Am. Mineral.* **52,** 1508–1514.

WILSON, E. B., J. C. DECIUS AND P. C. CROSS (1955) *Molecular Vibrations.* McGraw Hill, New York.

Manuscript received, March 23, 1976; accepted for publication, July 21, 1976.